Microporous and Mesoporous Materials 293 (2020) 109778

Contents lists available at ScienceDirect

Microporous and Mesoporous Materials

journal homepage: http://www.elsevier.com/locate/micromeso

Potential of triphenylphosphine as solid-state NMR probe for studying the noble metal distribution on porous supports

Michael Dyballa [a,*], Carolin Rieg [a], Daniel Dittmann [a], Zheng Li [a], Michael Buchmeiser [b], Bernd Plietker [c], Michael Hunger [a]

[a] Institute of Chemical Technology, University of Stuttgart, 70550, Stuttgart, Germany
[b] Institute of Polymer Chemistry, University of Stuttgart, 70550, Stuttgart, Germany
[c] Institute of Organic Chemistry, University of Stuttgart, 70550, Stuttgart, Germany

ARTICLE INFO

Keywords:
Mesoporous and microporous supports
Zeolite Y
Noble metal distribution
Triphenylphosphine
^{31}P MAS NMR spectroscopy

ABSTRACT

Triphenylphosphine (PPh_3) is demonstrated to be a useful molecular probe and tool for quantitatively characterizing the spatial distribution of noble metals on porous supports. The preparation of metal organic complexes by loading the supports with PPh_3 was performed by physically mixing the water-free catalysts with solid PPh_3 powder in nitrogen atmosphere and heating this mixture at 363 K for 20 h. Based on quantitative ^{31}P MAS NMR spectroscopy, the formation of noble metal (NM) tetrakis(triphenylphosphine) complexes $(PPh_3)_4NM$ on Pt- and Rh-containing silica and SBA-15 supports was evidenced. The large specific surface areas and mesopore diameters (3.4–4.5 nm) of these supports provide suitable conditions for the quantitative formation of $(PPh_3)_4NM$ complexes with a molecule size of ca. 2 nm. The micropores and cages of zeolites Y (0.72 and 1.14 nm, respectively), on the other hand, are too small for the formation of these complexes. Consequently, quantitative ^{31}P MAS NMR investigations of noble metal containing zeolites Y indicated that only 7% of the Pt and 6% of the Rh atoms are accessible for the complex formation with PPh_3. In other words, these noble metal quantities are located outside of the micropores and cages of the zeolite particles. The non-involved 93% of Pt and 94% of Rh atoms on the zeolites Y under study are located inside the micropores and cages of this support material, making them available for shape-selective heterogeneous catalysis.

1. Introduction

Understanding the properties of porous catalysts requires deep insights into the chemical properties of the catalytically active centres, their density, and their accessibility. Especially for shape-selective heterogeneous catalysis, the spatial distribution of the active centres is an important parameter strongly influencing the obtained product composition. For the spectroscopic characterization of the spatial distribution of Brønsted acid sites in pores and cages of solid catalysts, numerous probe molecules with different molecular sizes, e.g. ammonia, pyridine, trimethylphosphine, triphenylphosphine etc. and combinations thereof are utilized [see e.g. Refs. [1–5]]. Similarly, also the spatial distribution of the active sites of Lewis acidic solid catalysts can be investigated. Until now, however, no spectroscopic probe molecules exist for the study of the spatial distribution of metals inside the pores and at the outer surface of porous support materials. The application of such molecular probes would allow an improved characterization of metal-containing porous catalysts giving deeper insights into the reasons of their shape-selective properties [6–8].

Important requirements for the choice of suitable molecular probes for the investigation of metals on porous solids are: (i) the formation of stable metal organic complexes by coordination to the metals under study, (ii) a molecular size of the formed complexes allowing to distinguish between metals located inside and outside of pores and cages, (iii) a simple and good reproducible procedure for the application of theses molecular probes and the formation of the corresponding complexes, and (iv) suitable spectroscopic properties of the formed metal organic complexes allowing quantitative spectroscopic investigations with high accuracy.

The aim of the present work was to investigate the potential of triphenylphosphine (PPh_3) as molecular probe for platinum and rhodium on microporous and mesoporous support materials. For this purpose, microporous zeolite Y and mesoporous SBA-15 as well as silica, loaded with 0.5–4 wt % Pt or Rh, were utilized as noble metal-containing model

* Corresponding author.
E-mail address: michael.dyballa@itc.uni-stuttgart.de (M. Dyballa).

https://doi.org/10.1016/j.micromeso.2019.109778
Received 21 August 2019; Received in revised form 18 September 2019; Accepted 30 September 2019
Available online 3 October 2019
1387-1811/© 2019 Elsevier Inc. All rights reserved.

catalysts. According to Ref. [9], well dispersed Pt and Rh atoms on zeolite Y are mainly located inside the supercages with an inner diameter of 1.14 nm [10] or the much smaller sodalite cages (β-cages) with an inner diameter of 0.66 nm [11]. The supercages of zeolite Y are connected via 12-membered oxygen windows with an inner diameter of 0.74 nm [11]. Considering these structural parameters, metal organic complexes formed with PPh_3 (having a molecular diameter of 0.72 nm [12]) should allow to distinguish between noble metals located inside and outside of the pore system of zeolite Y. Coordination of PPh_3 to Pt atoms, e.g., is accompanied by the formation of tetrakis(triphenylphosphine)platinum ($(PPh_3)_4Pt$) [13]. Based on the triphenylphosphine diameter of 0.72 nm and a Pt–P distance of ca. 0.22 nm [14], the diameter of $(PPh_3)_4Pt$ complexes with tetrahedrally arranged PPh_3 ligands follows to 1.88 nm. Hence, this complex is too large for a formation inside the pore and cage system of zeolite Y. For Pt- and Rh-containing silica and SBA-15 with mesopore diameters between 3.4 and 4.5 nm, on the other hand, no steric limitation for the formation of metal organic complexes with a size of ca. 2 nm exists (see Scheme 1). The pore diameters and sizes are visualized in Scheme 1.

The spectroscopic investigation of the molecular probe PPh_3 and the formed metal organic complexes was performed by quantitative ^{31}P MAS NMR spectroscopy. The ^{31}P isotope has a natural abundance of 100%, and a nuclear spin of $I = ½$, which are very suitable prerequisites for a quantitative spectroscopic characterization with high sensitivity.

2. Experimental part

2.1. Sample preparation

Commercial silica AEROSIL®300 (Evonik, Hanau, Germany) with a specific surface area of 270–330 m^2/g and mesopore diameters of up to 4.5 nm [15] was used after calcination for 12 h at 823 K in synthetic air. The platinum loading of this silica was carried out by stirring 5 g of the silica material in 100 ml of demineralized water at 313 K for 2 h and subsequent addition of 1 M aqueous solution of ammonia until the pH value of the solution reached pH = 10. Then, an aqueous solution with calculated amounts of the platinum salt $[Pt(NH_3)_4]Cl_2{\cdot}xH_2O$ (ChemPur) or the rhodium salt $RhCl_3{\cdot}xH_2O$ (Alfa Aesar) was added dropwise. The solution was stirred at 313 K for another 18 h. Finally, the resulting solid was collected by filtration, washed with 1.5 l demineralized water, and dried under atmospheric conditions at 353 K for 12 h. The obtained samples with platinum and rhodium contents of 1.1 and 0.4 wt % were, after subsequent calcination and reduction, termed 1 Pt/silica and 0.5 Rh/silica, respectively.

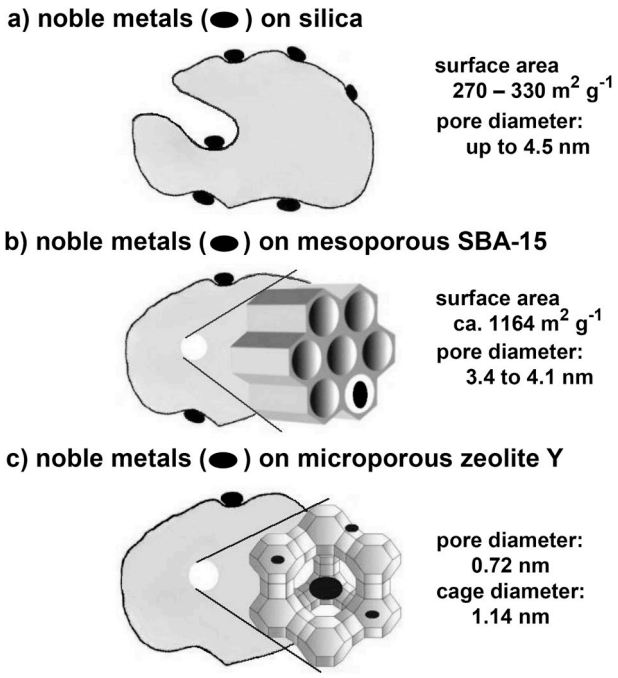

Scheme 1. Schematic depiction of the expected distribution of noble metal on silica (a), mesoporous SBA-15 (b), and FAU type zeolite Y (c). More details about morphological and structural parameters have been reported earlier [15].

The mesoporous SBA-15 with $n_{Si}/n_{Al} = 209$, a specific surface area of 1164 m^2/g, and mesopore diameters between 3.4 and 4.1 nm was synthesized as described by Zhao et al. [16]. The as-synthesized SBA-15 was heated with a rate of 2 K/min up to 823 K and calcined in air for 5 h to remove the template material. Subsequently, an incipient wetness impregnation with calculated amounts of the platinum salt $[Pt(NH_3)_4]Cl_2{\cdot}xH_2O$ (ChemPur) or the rhodium salt $RhCl_3{\cdot}xH_2O$ (Alfa Aesar) was performed. After stirring the solution for 5 min, the water was removed under vacuum at 313 K and the impregnated materials were dried under atmospheric conditions at 353 K for 12 h. The obtained samples with platinum and rhodium contents of 1.9 and 1.0 wt % were, after subsequent calcination and reduction, termed 2 Pt/SBA-15 and 1 Rh/SBA-15, respectively.

The commercially available dealuminated zeolite DeA-Y with $n_{Si}/n_{Al} = 93$ (Evonik, Hanau, Germany) and zeolite Na–Y with $n_{Si}/n_{Al} = 2.7$ (Evonik, Hanau, Germany) were stirred in 1 M aqueous solution of sodium nitrate at 353 K for 4 h and subsequently washed with demineralized water until nitrate-free. The purified zeolites DeA-Y and Na–Y were dried under atmospheric conditions at 353 K for 12 h. The noble metal-containing dealuminated zeolites DeA-Y were prepared by wetness impregnation using the same procedure like described for the noble metal-containing SBA-15. The obtained samples with platinum and rhodium contents of 4.6 and 1.8 wt % were, after subsequent calcination and reduction, termed 4 Pt/DeA-Y and 2 Rh/DeA-Y, respectively.

All noble metal-containing catalysts were calcined in synthetic air (750 ml/min) by heating with a rate of 2 K/min up to 573 K and calcination at this temperature for 3 h. Subsequently, these materials were reduced in flowing hydrogen (100 ml/min) at 623 K for 2 h, transferred into glass tubes inside a glove box under nitrogen atmosphere, evacuated ($p < 10^{-2}$ Pa) at 298 K for 12 h, and sealed air-tight.

The loading of triphenylphosphine (PPh_3) (Sigma-Aldrich, T84409-25g, Lot # WXBC006V) on the materials under study was performed by addition of 3–4 mg of dry PPh_3 to 40–50 mg of the dehydrated powder samples inside a 4 mm rotor. For loading with PPh_3, the metal-containing support materials were used as obtained after reduction and evacuation at room temperature (vide supra), while the pure support materials were dehydrated and evacuated ($p < 10^{-2}$ Pa) at 723 K for 12 h before their PPh_3 loading. For excluding contact to air, the PPh_3 loading was performed in a glove box purged with dry nitrogen. For a proper distribution of the added PPh_3 and the formation of metal organic complexes, the rotors filled with the sample mixture and closed with gas tight TORLON caps were heated at temperatures of 363–393 K for up to 40 h (see text for details).

The tetrakis(triphenylphosphine)platinum ($(PPh_3)_4Pt$) utilized as reference material was purchased from Sigma-Aldrich (216666-5G, Lot # SHBK0811). The zeolite H–Y utilized as Brønsted acidic reference material was obtained by a fourfold ion exchange of zeolite Na–Y (side supra) with an 1.0 M aqueous solution of NH_4NO_3 leading to an exchange degree of 91%. Subsequently, this NH_4^+ form zeolite Y was calcined, evacuated ($p < 10^{-2}$ Pa) at 723 K for 12 h to remove ammonia, and sealed in glass tubes. Zeolite-like material VPI-5 utilized as ^{31}P solid-state NMR intensity standard was synthesized as described by He and Klinowski [17]. For spectroscopic studies, the material was used in the hydrated state with a water content of 22.0 wt %.

2.2. Characterization methods

The chemical compositions of the noble metal-containing catalysts

under study were determined by optical emission spectroscopy (ICP-OES, Varian Vista-MPX). The structural intactness was proven by XRD (Bruker D8 diffractometer) and via ^{27}Al and ^{29}Si solid-state NMR spectroscopy (Bruker AVANCE III 400WB). BET surface areas were determined by physisorption of nitrogen (Autosorb-1, Quantachrome), while the metal dispersion was investigated by chemisorption of hydrogen using the same equipment and an assumed stoichiometry of 1 H atom per noble metal atom (Autosorb-1, Quantachrome).

All ^{31}P MAS NMR measurements were carried out on a Bruker Avance III 400WB spectrometer at the resonance frequency of 161.9 MHz using a 4 mm MAS NMR probe with sample spinning rates of 8 and 10 kHz. Spectra were recorded upon $\pi/2$ single-pulse excitation, high-power proton decoupling (HPDEC), and repetition times of 20–240 s for excluding saturation. Quantitative ^{31}P MAS NMR studies were performed by comparing the signal intensities of the samples under study with that of hydrated zeolite VPI-5 used as external intensity standard. The evaluation of the signal intensities was performed as described in literature for ^{1}H MAS NMR [4] under additional consideration of different receiver gain values (see also Section 3.3.). The simulation of the spinning sideband patterns of the ^{31}P MAS NMR spectra was performed using the Bruker software WINFIT.

3. Results and discussion

3.1. Interaction of PPh_3 with the pure support materials

For the investigation of the interaction of PPh_3 with the pure support surfaces and the effect of steric restrictions, dehydrated silica, SBA-15, and zeolites Y were loaded with the molecular probe. For this purpose, the dehydrated samples of these materials were mixed with PPh_3 and heated at 363 K for 5–12 h or 20 h inside gas-tight sealed MAS NMR rotors. The chosen temperature was slightly higher than the melting point of PPh_3 at 352–355 K [18]. The ^{31}P MAS NMR spectra of these samples are shown in Fig. 1. While bulk PPh_3 results in agreement with literature in a signal at $\delta = -9$ ppm (Fig. 2a) [19], adsorption of PPh_3 on silica and SBA-15 (Fig. 1a and 1b) is accompanied by a signal at $\delta = -6$ ppm. The latter resonance position agrees well with the one published by Hu and Gay [2,19], who observed ^{31}P MAS NMR signals between $\delta = -5.8$ and -6.4 ppm assigned to unreacted physisorbed PPh_3 on either a SiO_2 surface covering γ-Al_2O_3 particles or on pure γ-Al_2O_3, respectively. In the case of PPh_3 loaded on zeolite DeA-Y, which can also be considered as a siliceous support material ($n_{Si}/n_{Al} = 93$), up to three narrow signals at $\delta = -9$, -6, and -3 ppm occurred (Fig. 1c). According to the above-mentioned assignments, the first two of these signals are attributed to bulk PPh_3 and physisorbed PPh_3, respectively. As demonstrated by the ^{31}P MAS NMR spectra in Fig. S1, increasing heating time after adsorption of PPh_3 on zeolite DeA-Y is accompanied by an intensity increase of the signal at $\delta = -3$ ppm. Pure PPh_3 with the molecular diameter of 0.72 nm can enter the 12-membered oxygen windows of zeolite Y with the diameter of 0.74 nm. This assumption is supported by studies of Okumura et al. [20], who determined a PPh_3 adsorption capacity of zeolite Y of up to 1 mmol PPh_3 per gram at 373 K. Therefore, the above-mentioned increase of the signal at $\delta = -3$ ppm hints at a slow diffusion of PPh_3 into the micropore system, which is accompanied by a confinement effect [21]. This confinement of PPh_3 leads to a resonance shift from $\delta = -6$ ppm (PPh_3 adsorbed at the outer surface) to $\delta = -3$ ppm (PPh_3 adsorbed in micropores).

For clarifying the effect of extra-framework cations and Brønsted acid sites on the resonance positions of PPh_3 adsorbed on zeolite Y, this molecular probe was loaded on zeolites Na–Y and H–Y. According to the spectrum in Fig. 1d, interaction of PPh_3 with cationic sites, like extra-framework Na^+, causes a further low field shift of the ^{31}P MAS NMR signal to $\delta \cong$ 1 ppm. The broadening of the signal at $\delta \cong$ 1 ppm can be explained by the presence of Na^+ cations at different crystallographic positions inside the supercages (cation positions SII, SIII [11]) leading to slightly different adsorbate complexes. As observed for PPh_3 on zeolite DeA-Y, also PPh_3 on zeolite Na–Y requires suitable heating times for the diffusion into the zeolite cages and the coordination to the extra-framework Na^+ cations (see Fig. S2).

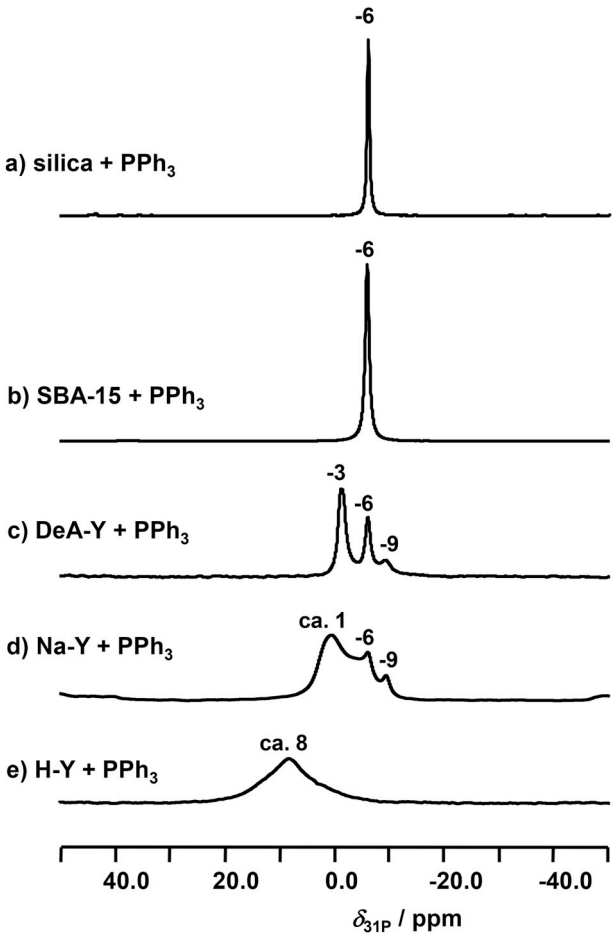

Fig. 1. ^{31}P MAS NMR spectra of PPh_3-loaded silica (a), mesoporous SBA-15 (b), and microporous zeolites DeA-Y (c), Na–Y (d), and H–Y (e) recorded after heating at 363 K for 20 h.

As demonstrated by Hu and Gay [19] and later Wang et al. [3] for PPh_3 adsorbed on acidic silica-alumina or zeolite H-MCM-22, respectively, protonation of PPh_3 (PPh_3H^+) is an additional source for a resonance shift of the ^{31}P MAS NMR signal (up to $\delta = 7.2$ ppm for silica-alumina and up to $\delta = 14.8$ ppm for MCM-22). In the case of PPh_3 loaded on zeolite H–Y, containing Brønsted acid sites in the supercages (see e.g. Refs. [4,22], this chemisorption process leads to a ^{31}P MAS NMR signal at $\delta = 8$ ppm (Fig. 1e).

In Table 1, upper part, a summary of the ^{31}P MAS NMR signals observed for PPh_3 interacting with the pure support materials is given. Based on these values it can be summarized that physisorption of PPh_3 on the support materials used in the present work can lead to physisorption-induced resonance shifts of the ^{31}P MAS NMR signals of up to 10 ppm. This resonance shift can be further increased in the presence of Brønsted acid sites due to chemisorption of PPh_3, i.e. the formation of PPh_3H^+. For excluding an overlap of ^{31}P MAS NMR signals due to formation of PPh_3H^+ and of metal organic complexes, a siliceous zeolite (zeolite DeA-Y with $n_{Si}/n_{Al} = 93$) was used as support material for further studies on noble metal-containing microporous model catalysts.

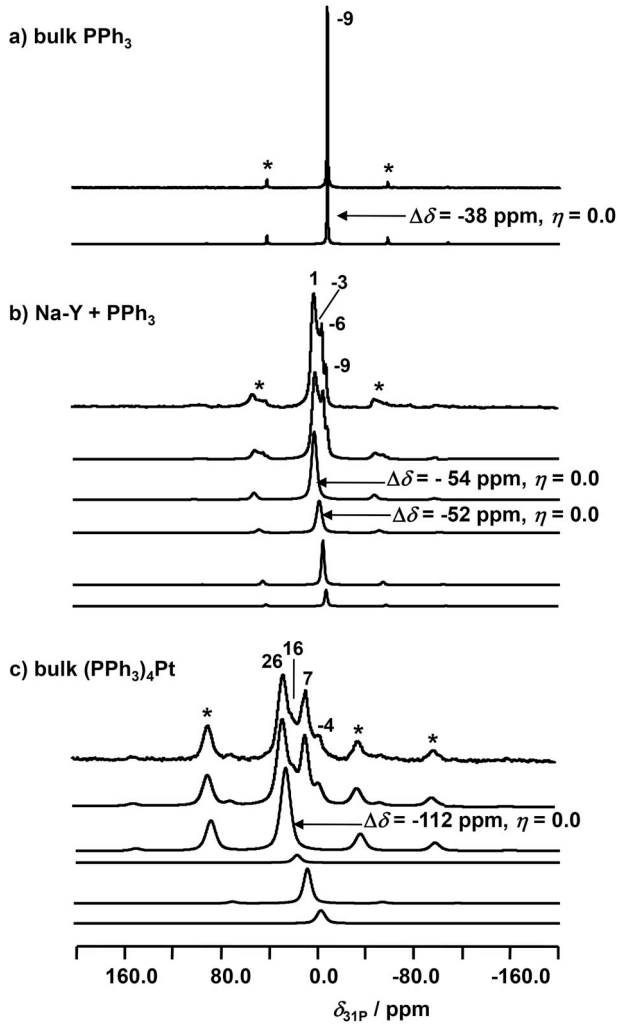

Fig. 2. ^{31}P MAS NMR spectra of bulk PPh_3 (a), zeolite Na–Y loaded with PPh_3 (b), and bulk tetrakis(triphenylphosphine)platinum (c) and their simulation for determining the chemical shift anisotropy $\Delta\delta$ and asymmetry parameter η by computer aided spinning sideband analysis. The spectra were recorded with sample spinning rates of $\nu_{rot} = 8$ (a, b) and 10 kHz (c). Asterisks denote spinning sidebands.

3.2. Formation of metal organic complexes by PPh_3 adsorption to noble metal-containing porous supports

For studying PPh_3-induced complex formation with supported noble metals, the materials studied in the former section were modified with platinum and rhodium (see Section 2.1.). Generally, the formation of metal organic complexes via coordination of PPh_3 with noble metals has to be accompanied by significant low field shifts of the ^{31}P MAS NMR signals. Bemi et al. [23], e.g., observed a signal at $\delta = 15$ ppm for tetrakis (triphenylphosphine)palladium, measured in the solid phase. For PPh_3-containing Rh complexes on SBA-15, Lan et al. [24] obtained ^{31}P MAS NMR signals at $\delta = 35.2$–36.5 ppm.

Furthermore, the formation of metal phosphine complexes is often accompanied by a significant increase of the chemical shift anisotropy $\Delta\delta$ of the ^{31}P solid-state NMR signals in relation to the value of this spectroscopic parameter for bulk PPh_3 [23]. According to the ^{31}P MAS NMR spectrum shown in Fig. 2a, bulk PPh_3 is characterized by a chemical shift anisotropy of $\Delta\delta = -38 \pm 4$ ppm (defined by $\Delta\delta = \delta_{zz} - (\delta_{xx} + \delta_{yy})/2)$) and an asymmetry parameter $\eta = 0.0$ (defined by $\eta = (\delta_{yy}\text{-}\delta_{xx})/(\delta_{zz}\text{-}\delta_{iso})$). Already an interaction of PPh_3 with extra-framework Na^+ cations in dehydrated zeolite Y is accompanied by an increase of the chemical shift anisotropy to $\Delta\delta = -54 \pm 5$ ppm. In the case of a coordination of PPh_3 to a noble metal, such as Pt, e.g. for solid $(PPh_3)_4Pt$, both these effects, i.e. low field resonance shift and increase of the chemical shift anisotropy, are much stronger. For $(PPh_3)_4Pt$, a low field ^{31}P MAS NMR signal at $\delta = 26$ ppm and a chemical shift anisotropy of $\Delta\delta = -112 \pm 11$ ppm were found (Fig. 2c). Hence, both the isotropic chemical shift δ and the chemical shift anisotropy $\Delta\delta$ are sensitive spectroscopic parameters for the assignment of metal organic complexes formed by PPh_3 with metal atoms supported on porous solids.

Table 1
Survey over ^{31}P MAS NMR signals and their assignments to the different kinds of PPh_3 species and phosphine complexes occurring on the porous support materials studied in the present work (NM: noble metal).

δ_{31P}/ ppm	Assignment	Observed for these Samples
−9	bulk PPh_3	PPh_3 (Sigma-Aldrich), DeA-Y, Na–Y, Pt/DeA-Y, Rh/SBA-15
−6	physisorbed PPh_3 on surface	silica, SBA-15, DeA-Y, Na–Y, and these NM modified supports
−3	physisorbed PPh_3 in zeolite cages	DeA-Y, Na–Y, Pt/DeA-Y, Rh/DeA-Y
ca. 1	PPh_3 coordinated at Na^+ ions in zeolite cages	Na–Y
6	decomposed $(PPh_3)_nPt$ complex	$(PPh_3)_4Pt$ (Aldrich)
8	protonated PPh_3 (PPh_3H^+)	H–Y
26	bulk $(PPh_3)_4Pt$	$(PPh_3)_4Pt$ (Aldrich), Pt/SBA-15, Pt/DeA-Y, Rh/DeA-Y
ca. 30	physisorbed $(PPh_3)_4Pt$	Pt/DeA-Y
ca. 30	physisorbed $(PPh_3)_4RhH$	Rh/DeA-Y
32	physisorbed $(PPh_3)_4Pt$	Pt/silica
34	physisorbed $(PPh_3)_4Pt$	Pt/silica, Pt/SBA-15
34	physisorbed $(PPh_3)_4RhH$	Rh/silica, Rh/SBA-15

As a prerequisite for reproducible quantitative studies of PPh_3 applied as a molecular probe for noble metals on porous solids, the conditions of complex formation, i.e. the temperature and time dependence, were investigated. Table 2 gives a survey on the samples and their noble metal loadings used for these and the subsequent experiments.

As representative examples, Fig. 3 shows the ^{31}P MAS NMR spectra of zeolite 4 Pt/DeA-Y and mesoporous 1 Rh/SBA-15 loaded with PPh_3. These spectra were recorded after heating of the with PPh_3 loaded samples at 393 K (top) and 363 K (bottom) for 12 h. While the spectra of the samples heated at 393 K show no (4 Pt/DeA-Y) and only weak signals (1 Rh/SBA-15) in the expected low field range of metal phosphine complexes, heating at 363 K led to much stronger signals at $\delta = 26$–34 ppm. Hence, a treatment temperature only slightly higher than the melting point of PPh_3 of 352–355 K [18] is more preferred for the complex formation, probably because higher temperatures shift the equilibrium to the side of complex degradation. The ^{31}P MAS NMR spectra in Fig. 4 show how heating time at 363 K influences the resulting spectra. As indicated by the intensities of the broad low field signals at 32–34 ppm, for both Pt and Rh on silica, a heating time of 20 h is more preferred for an optimum complex formation. No significant changes of

Table 2
Properties of the noble metals (NM) of the Pt- and Rh-containing samples under study.

Samples	NM Contents[a)] /wt.-%	NM Dispersions[b)] /%
1 Pt/silica	1.1	79
2 Pt/SBA-15	1.9	35
4 Pt/DeA-Y	4.6	14
0.5 Rh/silica	0.4	56
1 Rh/SBA-15	1.0	67
2 Rh/DeA-Y	1.8	83

[a)] Determined by ICP-OES (experimental accuracy ± 5%).
[b)] Determined by chemisorption of hydrogen with stoichiometry 1 H: 1 NM.

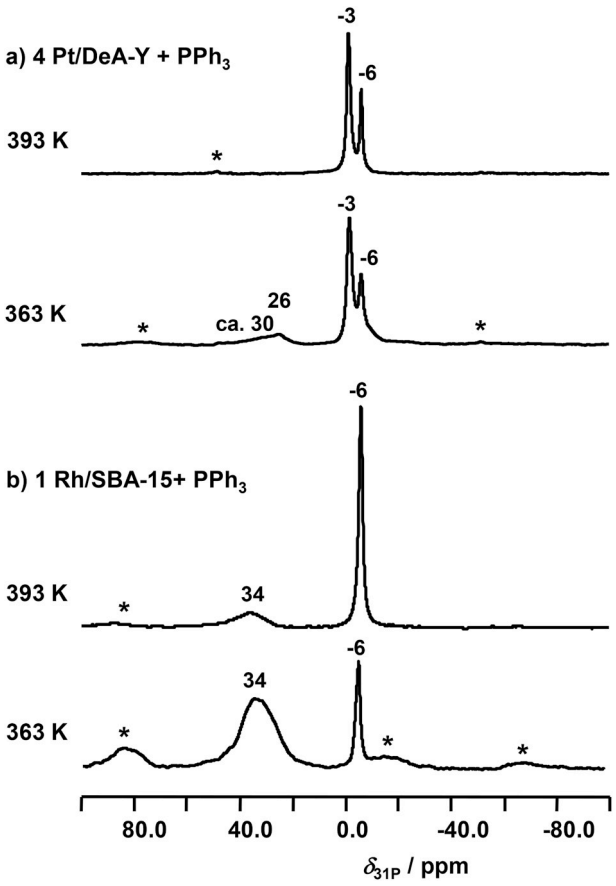

Fig. 3. ^{31}P MAS NMR spectra of PPh_3-loaded Pt-containing zeolite DeA-Y (a) and Rh-containing SBA-15 (b) recorded after heating at 393 K (top) and 363 K (bottom). Asterisks denote spinning sidebands.

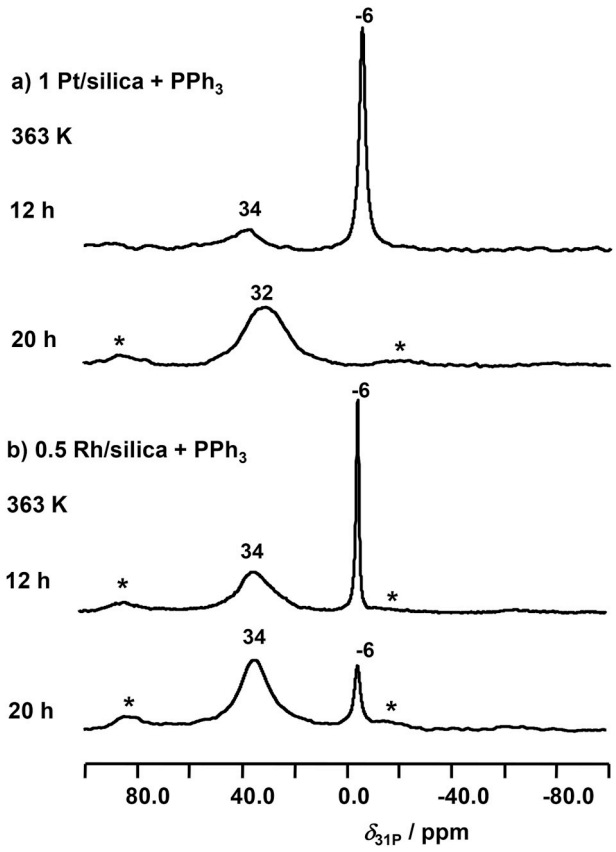

Fig. 4. ^{31}P MAS NMR spectra of PPh_3-loaded Pt-containing silica (a) and Rh-containing silica (b) recorded after heating at 363 K for 12 h (top) and 20 h (bottom). Asterisks denote spinning sidebands.

these low field signals were observed after prolonged heating for 40 h (not shown).

For supporting the assignment of the low field ^{31}P MAS NMR signals at $\delta = 26$–34 ppm, their chemical shift anisotropy $\Delta\delta$ was determined by a computer simulation of the sideband pattern. Fig. 5 shows the experimental ^{31}P MAS NMR spectra (top) of 2 Pt/SBA-15 and 1 Rh/SBA-15 both loaded with PPh_3, the sum spectrum of the theoretical spectra (middle) and the different signal components (bottom). For both Pt- and Rh-containing SBA-15, a significant increase of the chemical shift anisotropy ($\Delta\delta = -82$ to -98 ppm) was found in comparison with bulk PPh_3 ($\Delta\delta = -38$ ppm, Fig. 2a). The similarly large chemical shift anisotropy of bulk $(PPh_3)_4Pt$ ($\Delta\delta = -112$ ppm, Fig. 2c) is a strong argument to assign the low field signals in Figs. 3 and 4 to ^{31}P atoms in the metal phosphine complexes. Considering the resonance position of $(PPh_3)_4Pt$ of $\delta = 26$ ppm (Fig. 2c) and the physisorption-induced low field shift of up to 10 ppm observed for PPh_3 adsorbed on the pure support materials, also the isotropic chemical shifts of the low field ^{31}P MAS NMR signals at $\delta = 26$–34 ppm in Figs. 3 and 4 support their assignment to metal phosphine complexes. Furthermore, this range of low field signals is in reasonable agreement with the value of $\delta = 28.5$ ppm observed for the coordination of poly(tris(4-vinylphenyl) phosphine) to Pt nanoparticles [25] and the value of $\delta = 36.8$ ppm obtained for coordination of PPh_3 to Rh particles on SBA-15 [24]. In Table 1, lower part, a summary of the above-mentioned low field signals and their assignment is given. A survey on the assignment of the ^{31}P MAS NMR signals for each sample under study is given in Table S1.

3.3. Quantitative ^{31}P MAS NMR investigation of the metal distribution on porous catalysts

The quantitative investigation of the amount of metal phosphine complexes formed by coordination of PPh_3 to Pt and Rh dispersed on silica, SBA-15, and zeolite DeA-Y was performed using the well-defined ^{31}P MAS NMR spectrum of a zeolite VPI-5 as external intensity standard. After subtraction of the water content, this zeolite has 8.2 mmol ^{31}P atoms per gram material, determined by ICP-OES. For excluding saturation effects influencing the signal intensities, the reference VPI-5 was recorded with a repetition time of 120 s, leading to the same intensities than with a repetition time of 240 s. The noble metal-containing catalysts under study were recorded with a repetition time of 20 s and it was verified that the same intensities as with a repetition time of 120 s occurred.

Figs. 6 and 7 allow a comparison of the complex formation between PPh_3 and Pt or Rh dispersed on silica, SBA-15, and zeolite DeA-Y. All these noble metal-containing catalysts were loaded with PPh_3 according to the procedure described in Section 2.1. and subsequently heated at 363 K for 20 h. The evaluation of the intensities of the signals at $\delta = 26$–34 ppm was performed via the following equation:

$$c_P = 0.443 \cdot (57 / m_x) \cdot (A / 1000) \cdot 8.2\ \text{mmol g}^{-1} \quad (1)$$

with the concentration of ^{31}P atoms (c_P), the ratio of receiver gains used for recording VPI-5 and the sample under study (456/1030 = 0.443), the weight of water-free VPI-5 (57 mg), the weight of the sample under study (m_x in mg), the integral intensity of the sample under study (A) compared with this integral for VPI-5 (1000), and the concentration of ^{31}P atoms in water-free VPI-5 (8.2 mmol g^{-1}). The concentration of ^{31}P atoms contributing to the low field signals in Figs. 6 and 7, calculated via

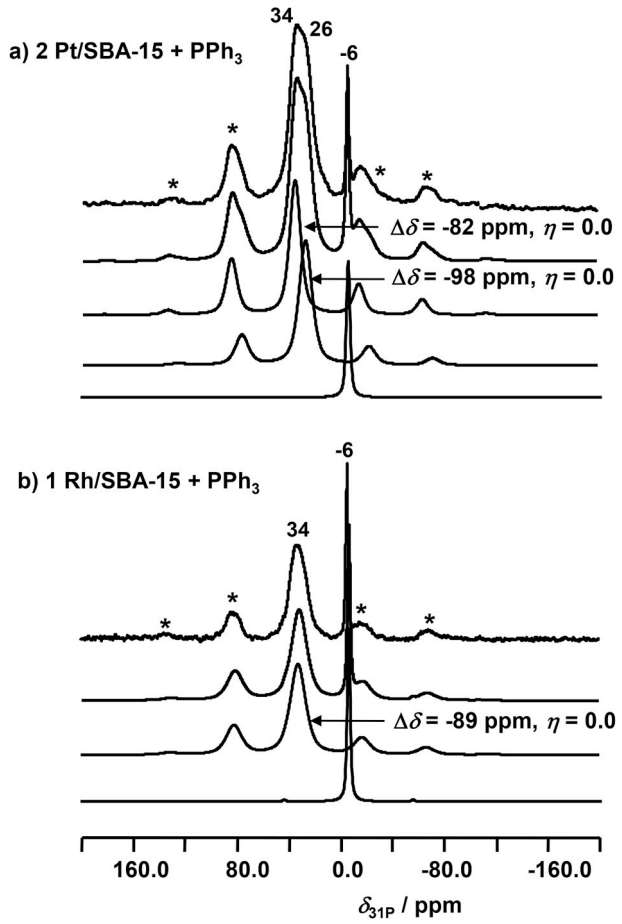

Fig. 5. ^{31}P MAS NMR spectra of PPh_3-loaded Pt-containing SBA-15 (a) and Rh-containing SBA-15 (b) and their simulation for determining the chemical shift anisotropy $\Delta\delta$ and asymmetry parameter η by computer aided spinning sideband analysis. The spectra were recorded with a sample spinning rate of $\nu_{rot} = 8$ kHz. Asterisks denote spinning sidebands.

Eq. (1), are summarized in Table 3, column 3. For comparison, the concentration of noble metals (NM) calculated via the noble metal contents given in Table 2, column 2, are given in Table 3, column 2.

Comparison of the values in Table 3, columns 2 and 3, for noble metal-containing silica and SBA-15, indicate that the number ^{31}P atoms in PPh_3 ligands and the number of noble metal atom have a ratio of ca. 4. This finding indicates that mainly $(PPh_3)_4NM$ complexes are formed by coordination of PPh_3 to Pt and Rh on these model catalysts. Assuming formation of $(PPh_3)_4Pt$ and, tentatively, hydridotetrakis(triphenylphosphine)rhodium $(PPh_3)_4RhH$ (Table 3, column 4), the contents of noble metals contributing to the formation of these complexes can be calculated. These contents, summarized in Table 3, column 5, indicate that nearly all noble metal atoms dispersed on silica and SBA-15 are accessible for PPh_3 and involved in the complex formation. For noble metals on zeolite Y, by contrast, this content is significantly lower, i.e. only 7% for 4 Pt/DeA-Y and 6% for 2 Rh/DeA-Y. Despite PPh_3 can enter the 12-membered oxygen windows of zeolite Y, it cannot form metal phosphine complexes inside the cages diameter of 1.14 nm of this microporous support material. Formation of this metal organic complex with a diameter of ca. 2 nm (see Section 1.) is exclusively possible for the noble metal atoms located at the outer surface of zeolites Y, which have the above-mentioned contents of 7% and 6%, respectively. Hence, noble metal atoms with contents of 93% for 4 Pt/DeA-Y and 94% for 2 Rh/DeA-Y are not available for a complexation with PPh_3, i.e. they are located within the micropores and cages of zeolite Y.

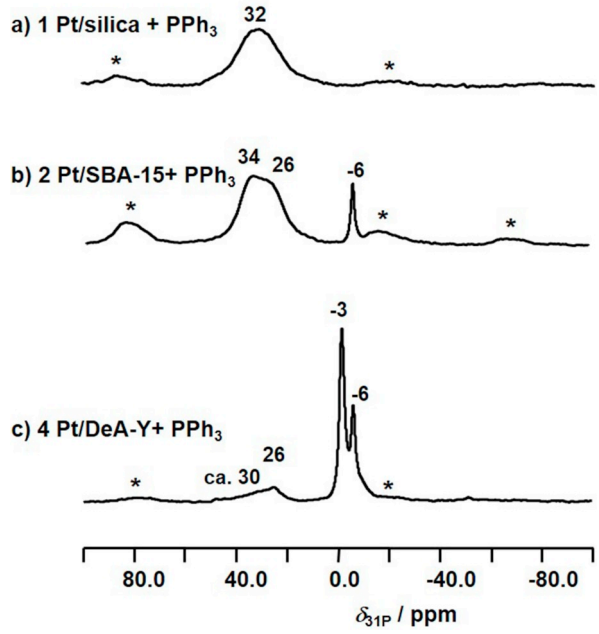

Fig. 6. ^{31}P MAS NMR spectra of PPh_3-loaded Pt-containing silica (a), SBA-15 (b), and zeolite DeA-Y (c) recorded after heating at 363 K for 20 h. Asterisks denote spinning sidebands.

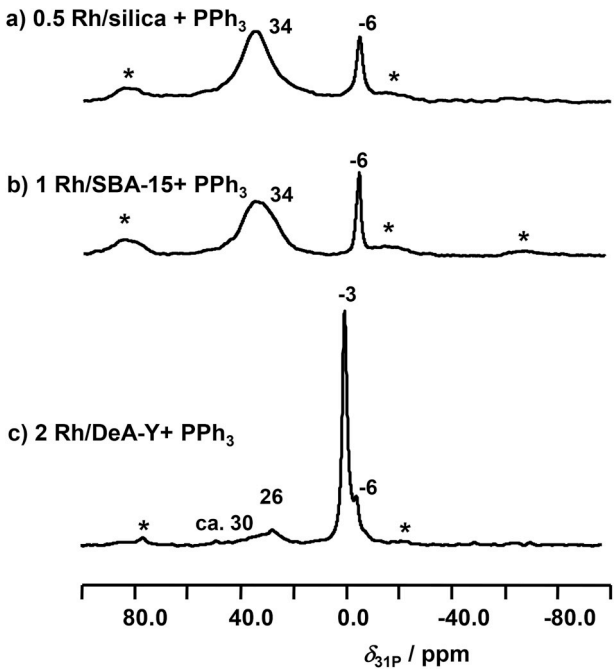

Fig. 7. ^{31}P MAS NMR spectra of PPh_3-loaded Rh-containing silica (a), SBA-15 (b), and zeolite DeA-Y (c) recorded after heating at 363 K for 20 h. Asterisks denote spinning sidebands.

4. Conclusion

The present work demonstrates that the formation of metal phosphine complexes after reaction of PPh_3 with noble metals (NM) supported on porous solids can be quantitatively studied with high accuracy by ^{31}P MAS NMR spectroscopy. A simple method for the preparation of metal phosphine complexes, which consists of a physical mixture of the water-free samples under study with solid PPh_3 powder inside a glove box and a heating of this mixture at 363 K for 20 h, was tested and

Table 3
Results of the ^{31}P MAS NMR studies of the PPh_3-loaded noble metal-containing (NM) model catalysts investigated in the present work.

Samples	NM loadings[a)] /μmol g^{-1}	^{31}P in PPh_3 complexes[b)] /μmol g^{-1}	$(PPh_3)_4NM$ complexes[b)] /μmol g^{-1}	NM bound in $(PPh_3)_4NM$ complexes[a,b)] /%
1 Pt/silica	56.4	215.6	53.9	95.6
2 Pt/SBA-15	97.4	404.4	101.1	103.8
4 Pt/DeA-Y	235.8	67.3	16.8	7.1
0.5 Rh/silica	38.9	156.8	39.2	100.8
1 Rh/SBA-15	97.2	371.0	92.7	95.4
2 Rh/DeA-Y	174.9	44.0	11.0	6.3

[a)] Determined by ICP-OES (experimental accuracy ± 5%).
[b)] Determined by quantitative ^{31}P MAS NMR (experimental accuracy ± 10%).

demonstrated.

Two NMR spectroscopic parameters are available for the assignment of such complexes: (i) an isotropic chemical shift in the range of $\delta = 26$–34 ppm and (ii) an enhanced chemical shift anisotropy of $\Delta\delta = -80$ to -110 ppm. Quantification of the ^{31}P MAS NMR signals of metal organic complexes formed by coordination of PPh_3 to Pt and Rh can be performed via an external intensity standard (e.g. zeolite-like material VPI-5). Due to the spin of $I = ½$ of the ^{31}P nuclei and their 100% natural abundance, this quantification is possible with high accuracy and sensitivity.

Based on the spectroscopic parameters isotropic chemical shift and chemical shift anisotropy and by taking into account the quantified concentration of PPh_3 species, it was evidenced that noble metal (NM = Pt, Rh) complexes with the stoichiometry $(PPh_3)_4NM$ were formed on noble metal-containing silica and SBA-15. The outer surface and mesopore diameters of silica and SBA-15 support materials provide suitable conditions for the formation of these complexes characterized by a diameter of ca. 2 nm. In contrast, the micropores and cages of zeolites Y are too small for the formation of $(PPh_3)_4NM$ complexes. Consequently, only 7% and 6% of the Pt and Rh atoms, respectively, on the zeolite Y samples under study were found to contribute to the complex formation with PPh_3. Hence, the majority, i.e. 93% and 94% of the noble metal atoms are located inside the micropores and cages of this support material and are therefore available for shape-selective heterogeneous catalysis. Based on these results, the present investigations demonstrate that PPh_3 is a powerful molecular probe and useful tool for quantitatively characterizing the spatial distribution of noble metals dispersed on porous catalysts.

Acknowledgements

We thank Ann-Katrin Beurer, Marvin Stoll, Dorothea Häussermann, and Heike Fingerle (all University of Stuttgart) for nitrogen adsorption studies and ICP-OES measurements. The authors gratefully acknowledge funding by the Deutsche Forschungsgemeinschaft (DFG, German Research Foundation) under project number 358283783 (CRC 1333).

Appendix A. Supplementary data

Supplementary data to this article can be found online at https://doi.org/10.1016/j.micromeso.2019.109778.

References

[1] J.H. Lunsford, W.P. Rothwell, W. Shen, J. Am. Chem. Soc. 107 (1985) 1540–1547.
[2] B. Hu, I.D. Gay, J. Phys. Chem. B 105 (2001) 217–219.
[3] Y. Wang, J. Zhuang, G. Yang, D. Zhou, D. Ma, X. Han, X. Bao, J. Phys. Chem. B 108 (2004) 1386–1391.
[4] Y. Jiang, J. Huang, W. Dai, M. Hunger, Solid State Nucl. Magn. Reson. 39 (2011) 116–141.
[5] A. Zheng, S.-B. Liu, F. Deng, Solid State Nucl. Magn. Reson. 55–56 (2013) 12–27.
[6] R.M. Dessau, J. Catal. 89 (1984) 520–526.
[7] J. Weitkamp, S. Ernst, L. Puppe, J. Weitkamp, L. Puppe, Catalysis and Zeolites, Springer-Verlag, Berlin, 1999, p. 367.
[8] S. Ernst, G. Ertl, H. Knözinger, F. Schüth, J. Weitkamp, Handbook of Heterogeneous Catalysis, Wiley-VCH, Weinheim, 2008, p. 626.
[9] W.J. Mortier, Compilation of Extra Framework Sites in Zeolites, Butterworth Scientific Limited, Westbury, UK, 1982, pp. 19–31.
[10] J.M. Newsam, Science 231 (1986) 1093–1099.
[11] D.W. Breck, Zeolite Molecular Sieves, reprinted), Krieger Publishing Company, Malabar, Florida, USA, 1984, p. 84, 96.
[12] J. Hjortkjaer, M.S. Scurrell, P. Simonsen, H. Svendsen, J. Catal. 12 (1981) 179–195.
[13] R. Ugo, F. Cariati, G. La Monica, Inorg. Synth. 11 (1968) 105–108.
[14] P.G. Waddell, A.M.Z. Slawin, J.D. Woollins, Dalton Trans. 39 (2010) 8620–8625.
[15] U. Obenaus, S. Lang, R. Himmelmann, M. Hunger, J. Phys. Chem. C 121 (2017) 9953–9962.
[16] D. Zhao, J. Feng, Q. Huo, N. Melosh, G.H. Fredrickson, B.F. Chmelka, G.D. Stucky, Science 279 (1998) 548–552.
[17] H. He, J. Klinowski, J. Phys. Chem. 98 (1994) 1192.
[18] G.G. Hawley, The Condensed Chemical Dictionary, eighth ed., Van Nostrand Reinhold Company, New York, 1971, p. 900.
[19] B. Hu, I.D. Gay, Langmuir 15 (1999) 477–481.
[20] K. Okumura, K. Okazaki, H. Yamashita, Y. Koga, Microporous Mesoporous Mater. 268 (2018) 285–292.
[21] M. Gackowski, J. Podobinski, M. Hunger, Microporous Mesoporous Mater. 273 (2019) 67–72.
[22] M. Hunger, Catal. Rev. Sci. Eng. 39 (1997) 345–393.
[23] L. Bemi, H.C. Clark, J.A. Davies, C.A. Fyfe, R.E. Wasylishen, J. Am. Chem. Soc. 104 (1982) 438–445.
[24] X. Lan, W. Zhang, L. Yan, Y. Ding, X. Han, L. Lin, X. Bao, J. Phys. Chem. C 113 (2009) 6589–6595.
[25] S. Jayakumar, A. Modak, M. Guo, H. Li, X. Hu, Q. Yang, Chem. Eur J. 23 (2017) 7791–7797.